Proc. Natl. Acad. Sci. USA
Vol. 91, pp. 1873–1877, March 1994
Genetics

Efficient detection of point mutations on color-coded strands of target DNA

(DNA diagnosis/mismatch analysis/fluorescent PCR/C1-inhibitor deficiencies)

E. VERPY, M. BIASOTTO, T. MEO, AND M. TOSI*

Unité d'Immunogénétique et Institut National de la Santé et de la Recherche Médicale U.276, Institut Pasteur, 25, rue du Docteur Roux, 75724, Paris, France

Communicated by Jean Dausset, October 11, 1993 (received for review July 2, 1993)

ABSTRACT **Presently available methods for screening large genetic regions for unknown point mutations are neither flawless nor particularly efficient. We describe an approach, especially well suited to identifying mutations present in the heterozygous state, that combines several improvements in a protocol called fluorescence-assisted mismatch analysis (FAMA). Appropriate gene regions of the wild-type and the putative mutant allele are simultaneously amplified from genomic DNA by using the polymerase chain reaction, and large DNA fragments, so far up to 800 bp, are end labeled with strand-specific fluorophores. Aliquots are denatured and reannealed to form heteroduplexes and subjected to conventional cytosine- and thymine-specific modifications. Cleavages occurring on opposite strands are detected by denaturing gel electrophoresis using an automated DNA sequencer. Since the DNA fragments derived from the mutant allele are also end labeled, the number of informative mispaired bases is doubled compared to conventional searches using wild-type probes. The sensitivity of detection is also increased, because differential fluorescent end labeling allows the identification and measurement of strand-specific background cleavages at matched cytosine or thymine residues. Automatic superimposition of tracings from different subjects allows mismatch detection at sites that, because of the nature of the bases involved and of the neighboring sequence, are known to be less susceptible to cleavage. The effects of the latter parameters have been studied quantitatively on a series of point mutations found in the human C1-inhibitor gene in patients affected by hereditary angioedema. Dilution experiments have demonstrated that most mutations are detected even when the mutant chromosome is diluted 10-fold or more compared with the normal one.**

The identification of loci responsible for a large number of monogenic diseases and of a growing number of genes involved in tumor predisposition and multifactorial diseases has rapidly expanded the range of application of DNA diagnosis. Since the majority of inherited disorders are heterogeneous at the gene level and are more often due to subtle changes affecting one or several nucleotides than to large deletions or duplications, considerable efforts have been made to develop methods able to detect not only mutations previously identified in probands or known to be prevalent in a given population but also as yet unknown mutations (for reviews, see refs. 1–3). Each of the methods has, however, disadvantages that render its use problematic when searching unknown point mutations within large DNA regions. Denaturing gradient gel electrophoresis (4–6) requires, for example, computer-assisted optimization of the target region and of the electrophoresis conditions, depending on the sequence content of the DNA fragment. The single-strand conformation polymorphism technique (7), in spite of its experimental simplicity, has shown limited sensitivity for the detection of mutations in DNA fragments longer than 200 bp (8, 9). Neither of these methods, moreover, yields information as to the precise localization of the mutation within the DNA fragment under investigation. Direct sequencing methods, while improving rapidly, will probably remain costly and time consuming, when screening for unknown mutations, and have not been proven adequate to resolve unambiguously heterozygous point mutations, without further labor-intensive analyses.

The chemical cleavage of mismatch method (CCM) (10) is, in principle, well suited to detect mutations independently of the length and sequence composition of the region examined and has been used successfully in a large number of studies (refs. 11–16; reviewed in ref. 3). In the conventional CCM method, however, heteroduplexes are formed between enzymatically amplified DNA from the patient and a radioactively end-labeled fragment representing the wild-type sequence. Heteroduplex DNA molecules are produced with the wild-type sequence end labeled on the coding and the noncoding strand, respectively, and are chemically processed in parallel reactions in order to reveal mismatches. Theoretically, using two probes, all mutations should be detected after induction of cytosine-specific and thymine-specific modifications by hydroxylamine and osmium tetroxide since in all cases an unpaired C or T must be present at the site of the mutation, either in the coding or in the noncoding strand of the radioactively labeled probe. In practice, some mismatches are poorly cleaved, due to the nature of the unpaired bases and to the properties of their local sequence environment.

Additional possibilities of detection should be generated by simultaneous end labeling the PCR products corresponding to the wild-type sequence and those derived from the mutant allele, because of modification and cleavage at C or T residues introduced by the mutation into the coding or the noncoding strand of the mutant allele. Inherited diseases in which the mutation is heterozygous provide a convenient source of material to test this approach. Our efforts to develop an efficient procedure for searching unknown point mutations within large gene segments were prompted by our interest in the molecular bases of the autosomal dominant disease hereditary angioedema. This disease is caused by a variety of defects of the C1-inhibitor gene (17), which encodes a serine protease inhibitor that controls the activation of several plasma proteases.

MATERIALS AND METHODS

DNA Samples. We reexamined 37 unrelated hereditary angioedema patients who had not revealed C1-inhibitor gene alterations in previous DNA blot analyses (18). Initially, we screened the same DNA samples for point mutations in exon

The publication costs of this article were defrayed in part by page charge payment. This article must therefore be hereby marked "*advertisement*" in accordance with 18 U.S.C. §1734 solely to indicate this fact.

Abbreviations: CCM, chemical cleavage of mismatches; FAMA, fluorescence-assisted mismatch analysis.

*To whom reprint requests should be addressed.

8 by using the conventional version of CCM (10) and DNA sequencing.

Generation of Fluorescence-Labeled Template. One microgram of genomic DNA isolated from peripheral white blood cells was used for 30 or 35 cycles of PCR amplification in a 100-μl reaction with oligonucleotide primers E1 and E2, as illustrated in Fig. 1*A*. The fluorescence-labeled template was generated by reamplifying, typically for 25 cycles, 2 μl of the first amplification reaction using the same primers rendered fluorescent by coupling a dye-*N*-hydroxyl succinimide ester to an aminohexyl linker attached onto the 5′ end, according to the Applied Biosystems protocol. The sequence of oligonucleotide E1 (labeled with the JOE fluorophore) is 5′-GTGAACTTGAACTAGAGAAAGC-3′. The sequence of oligonucleotide E2 (labeled with the FAM fluorophore) is 5′-TGAGGATCCCACGAACTGCCAG-3′. Nested PCR was used for other gene segments.

Heteroduplex Formation and CCM. The basic protocol for chemical cleavage of mismatches has been described (10). Bichrome PCR fragments were ethanol precipitated, and 450 ng was boiled for 5 min in 150 μl of 0.3 M NaCl/3.5 mM $MgCl_2$/3 mM Tris·HCl, pH 7.7, annealed from 2 hr to overnight, ethanol precipitated, and resuspended in 18 μl of water. The annealing temperature was usually 42°C, but higher temperatures were used in some experiments. Six microliters of DNA was treated at 37°C for 45 min or 1 hr with 20 μl of a freshly prepared 7 M hydroxylamine hydrochloride (Merck) solution titrated to pH 6.0 by addition of diethylamine (Fluka). The final hydroxylamine concentration was ≈3.8 M. Osmium tetroxide [Aldrich; 4% (wt/vol) in water] was diluted in distilled water to give a 1% stock solution, and aliquots were stored at −80°C in siliconized tubes. Six microliters of DNA was incubated for 15 min at room temperature in 0.4% osmium tetroxide/2% pyridine (Aldrich)/5 mM Hepes, pH 8/0.5 mM Na_2 EDTA in a total volume of 25 μl using siliconized tubes. Modification reactions were terminated by transferring the samples to ice and adding 200 μl of 0.3 M sodium acetate, pH 5.2/0.1 mM Na_2 EDTA/yeast tRNA (50 μg/ml), and the nucleic acids were ethanol precipitated twice in a dry ice/ethanol bath. Pellets were resuspended in 50 μl of 1 M piperidine (Aldrich) and incubated at 90°C for 20 min. Five micrograms of yeast tRNA and 50 μl of 0.6 M sodium acetate (pH 6.0) were added, and the nucleic acids were ethanol precipitated. Pellets were resuspended in 100 μl of distilled water, lyophilized, and dissolved in 8 μl of 83% (vol/vol) formamide/8.3 mM Na_2 EDTA. Four microliters of each sample, mixed with 0.5 μl of fluorescent-labeled size standards (GS2500P ROX; Applied Biosystems), was loaded on a 6% denaturing polyacrylamide gel in an Applied Biosystems automated DNA sequencer. Data were collected and analyzed using the GENESCAN 672 (Applied Biosystems) software.

Safety Considerations. OsO_4 and piperidine are handled under a fume hood. The supernatants of both ethanol precipitations after OsO_4 modification are collected for safe disposal.

RESULTS

The C1-inhibitor gene is 17 kb long and is composed of eight exons (20). By choosing oligonucleotide primers in introns and in the 5′ or 3′ flanking regions of the gene, one obtains by PCR amplification a set of 600–1000-bp-long DNA fragments encompassing either individual exons or groups of them and covering all intron–exon boundaries.

Exon 8 was amplified with primers E1 and E2 as shown in Fig. 1*A*. E1 is located within the 3′ untranslated region, 211 bp downstream of the stop codon. E2 is located within intron 7, 147 bp upstream of the first nucleotide of exon 8. By using the conventional CCM technique to screen the DNA of

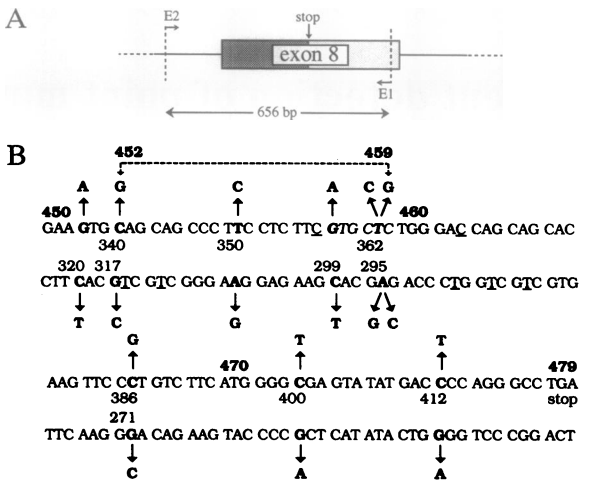

C

mutation	mismatch	% cleavage Exp1	Exp2	mutation	mismatch	% cleavage Exp1	Exp2
	HYDROXYLAMINE				OSMIUM TETROXIDE		
Arg472stop	GGGG^{C}GAGT CCCC$_{A}$CTCA	24	21	Arg472stop	GGGG^{T}GAGT CCCC$_{G}$CTCA	<1	<1
Val458Met	CTTC^{A}TGCT GAAG$_{C}$ACGA	40	34	Val458Met	CTTC^{G}TGCT GAAG$_{T}$ACGA	9	4
Val451Met	TGAA^{A}TGCA ACTT$_{C}$ACGT	43	40	Pro476Ser	TGAC^{T}CCAG ACTG$_{G}$GGTC	10	8
Phe455Ser	CCCT^{C}CCTC GGGA$_{A}$GGAG	50	53	Phe455Ser	CCCT^{T}CCTC GGGA$_{G}$GGAG	ND	8
Leu459Arg	GTGC^{T}CTGG CACG$_{C}$GACC	57	49	Leu459Pro	GTGC^{T}CTGG CACG$_{G}$GACC	23	11
Pro476Ser	TGAC^{C}CCAG ACTG$_{A}$GGTC	56	58	Val451Met	TGAA^{G}TGCA ACTT$_{T}$ACGT	34	19
Leu459Pro	GTGC^{C}CTGG CACG$_{A}$GACC	61	62	Leu459Arg	GTGC^{T}CTGG CACG$_{C}$GACC	43	31
Gln452Glu	AGTG^{C}AGCA TCAC$_{C}$TCGT	67	66	----------→	AGTG^{C}AGCA TCAC$_{C}$TCGT		
Pro467Arg	TTCC^{C}TGTC AAGG$_{C}$ACAG	82	79	----------→	TTCC^{C}TGTC AAGG$_{C}$ACAG		
Pro467Arg	TTCC^{C}TGTC AAGG$_{C}$ACAG	84	84				
Gln452Glu	AGTG^{C}AGCA TCAC$_{C}$TCGT	100	89				

FIG. 1. Point mutations detected in the last exon of the human C1-inhibitor gene. (*A*) Schematic presentation of the region, encompassing the coding portion of exon 8, that was amplified enzymatically from patients. (*B*) Mutations detected by conventional CCM and sequence analyses and reexamined using fluorescence-assisted mismatch analysis (FAMA). Nucleotide changes are shown with boldfaced letters above the coding and below the noncoding strand. Boldfaced numbers above triplets refer to codons of the C1-inhibitor protein (19). Numbers below the coding strand and above the complementary one mark the distance from the corresponding fluorescent end label. A double point mutation found in one patient is marked with arrows connected by a dotted line. An *Hgi*AI restriction site, which is polymorphic, due to the presence of a G or an A at the Val/Met codon 458 (19) is shown in italics. (*C*) Quantitative analysis of the reactivity of C or T residues with hydroxylamine and osmium tetroxide, respectively. Percentages in the columns Exp1 and Exp2 are from two sets of modification and cleavage. Since the cleavable mispaired base is expected to be present only on a quarter of the duplex molecules, these percentages were calculated as the ratios of the fluorescence of the corresponding cleavage product versus one-fourth the fluorescence in total DNA. When the same strand was cleaved at two sites, this ratio was corrected for the effect of the proximal cleavage on the observed intensity of the distal one. Arrows point to cleavages readily detected at adjacent residues. Mismatches above the dotted line could only be detected by superimposing tracings (see an example in Fig. 3).

patients, we found eight different point mutations in this area, most of which result in profound impairments of the production of the C1-inhibitor protein (E.V., unpublished data). In addition, a G → A transition within codon 458 generates a polymorphism for the restriction enzyme *Hgi*AI (19). In one patient, two mutations, at codon 452 (C → G) and at codon 459 (T → G), connected with a dotted line in Fig. 1*B*, were found on the same chromosome (data not shown). DNA from this patient was therefore used to identify the partial cleavage conditions that would allow detection of multiple mismatches. As shown in Fig. 2*A*, hydroxylamine cleavage of unpaired C residues on the noncoding strand (green) yields two peaks, at positions corresponding to the sizes of 295 nt and 317 nt, respectively, as predicted for the types of heteroduplex molecules expected. Both peaks are strong, relative to the fluorescence intensity of the uncleaved material. One should note in fact that only one-fourth of the DNA molecules are expected to contain the proper mismatch that renders these C residues readily accessible to hydroxylamine. These data, and similar data obtained with OsO_4 modifications, indicate that our conditions allow detection of multiple cleavages on the same strand. Slightly milder conditions of hydroxylamine treatment were subsequently used because cleavage at the distal position (peak 317), when corrected for the amount of fluorescence subtracted by the proximal cleavage, turned out to approach 100%. Fig. 2 also illustrates the redundancy of information obtained by labeling the products corresponding to both alleles. In this example, two mutations are revealed by a total of seven distinct cleavages. Among these, three have occurred at paired bases, adjacent to the mismatch—namely, on the coding strand, the C residues that yield weak but significant hydroxylamine peaks (discussed below) around position 362 and, on the noncoding strand, the T residue that yields the OsO_4 peak at position 316. Such cleavages at adjacent paired bases, although usually weaker than those at the mismatched residues themselves, may occur in half of the duplexes, rather than only in a quarter, as is typically the case for T- or C-containing mismatches (see the schematic diagram in Fig. 2). The gain in detection sensitivity provided by the use of differential labeling of each DNA strand combined with computerized analysis is illustrated in Fig. 2*A Inset*, which shows an enlargement of the doublet peaks around the destabilizing mutation at position 362 of the coding strand, superimposed onto the tracings of the same strand from three individuals lacking this mutation.

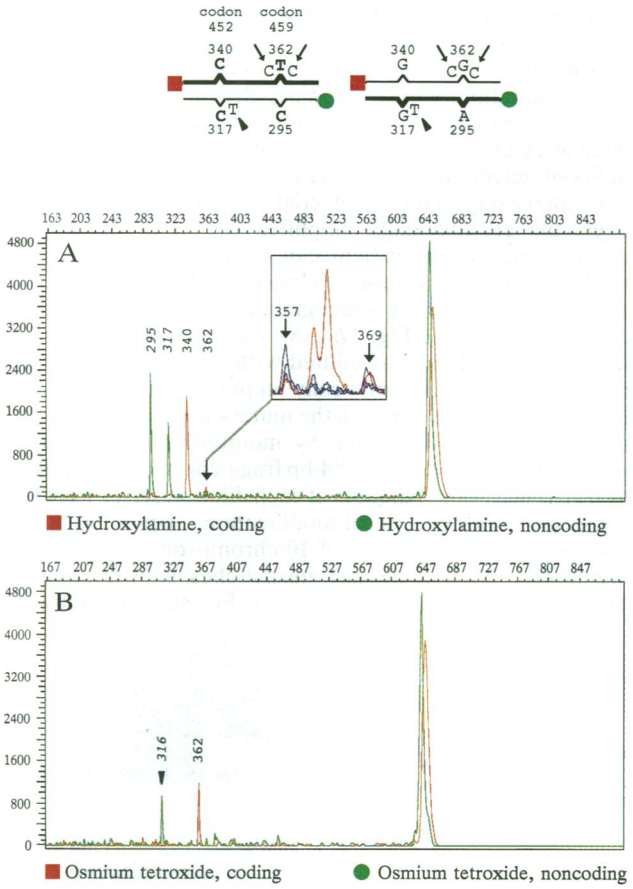

FIG. 2. Detection of multiple mutations. The schematic diagram depicts the heteroduplex molecules formed upon denaturation/renaturation of the amplified DNA from a patient with a cis double point mutation (see the arrows connected by a dotted line in Fig. 1*B*). For convenience, the FAM fluorophore at the 5′ end of the coding strand is indicated in red. The strands derived from the wild-type allele are marked with thick lines, and distances of the mispaired bases from the terminal fluorescent label are indicated. (*A*) Hydroxylamine modifications to reveal mispaired C residues. The size scale in nucleotides at the top of the diagram was obtained from the internal size marker, labeled with the ROX fluorescent dye (Applied Biosystems). The vertical scale indicates the intensities of fluorescence in arbitrary units. (*Inset*) Enlargement of the profile of the coding strand (red) between positions 357 and 369 from the terminal dye. It illustrates the detection of paired C residues, marked by arrows in the schematic diagram, which are immediately adjacent to mispaired bases. Cleavage at these C residues (red profile) is significantly stronger than that at other paired C residues, as revealed by comparison with three individuals not carrying the mutation (blue profiles). (*B*) Detection of cleavage at T residues using OsO_4. The arrowhead points to a paired T residue, adjacent to the mismatches at codon 452, which undergoes a rather strong cleavage (see the OsO_4 column in Fig. 1*C*). Note that adjacent cleavages occur on half of the duplexes.

The nine mutations shown in Fig. 1*B* allowed us to examine quantitatively the effect of the type of unpaired bases and of the composition of the neighboring bases on the susceptibility to chemical modification. As shown in Fig. 1*C*, these comparisons, based on two independent experiments, yield a reproducible hierarchy of cleavage susceptibilities. While the cleavage efficiencies obtained with hydroxylamine are consistently higher than those obtained with OsO_4, the nucleotide environment of the mismatch appears to have a similar effect on the susceptibility to both chemical modifications, since a similar order of cleavage efficiencies was observed with both reagents. A few mutations do not follow this rule. For example, Pro476Ser and Leu459Pro are relatively more susceptible to hydroxylamine modification, but this is probably due to the presence, in both cases, of three consecutive C residues at the site of cleavage. Similarly, the relatively high levels of OsO_4 cleavage of the Val451Met heteroduplexes are probably due to the presence of two consecutive T residues adjacent to the mispaired T. However, C·C mismatches stand out for their high susceptibility to modification even when embedded in two different nucleotide environments. This is documented not only by the strong hydroxylamine cleavage but also by the strong cleavage observed with OsO_4 at the immediately adjacent T residues. While T·G mismatches are sometimes detected inefficiently in the OsO_4 reactions (3), all six T·G mismatches in our series were detected, including that which results from the mutation Arg472stop and displays a T embedded within G residues. In line with the reported unreactivity of T residues immediately 3′ of a G base (discussed in refs. 14 and 21), this T was cleaved at a level even lower than that characteristic of paired T residues. It was however recognized upon comparison with the OsO_4 profile of other lanes (data not shown). One should note however that mutations leading to the formation of T·G mismatches are easily detected because of the complementary C·A mismatch, readily revealed by the hydroxylamine reaction.

Each of the mutations listed in Fig. 1*C* yielded at least two detectable fluorescent peaks resulting from cleavage at mispaired bases, but in several cases additional information was obtained from cleavage at adjacent paired positions, marked with arrows. The majority of cleavage products were readily detected, because the intensity of their fluorescent signal was clearly above the background. Superimposition of tracings such as the one shown in Fig. 2*A Inset* was necessary only for detection of signals representing <10% of the cleavable duplexes, such as the ones obtained by OsO_4 modification of the mismatches resulting from the Arg472stop and the Val458Met mutations. The OsO_4 profile of a patient heterozygous both for the latter mutation, which is an innocent polymorphism (19), and for the pathogenic Pro467Arg mutation (E.V., unpublished results) is illustrated in Fig. 3. The polymorphism at codon 458 was readily detected in the hydroxylamine lane (not shown) as a peak at position 299 of the noncoding strand, and the mutation at codon 467 (C → G) yielded the expected cleavage products on the coding and the noncoding strand in the hydroxylamine reaction (see Fig. 1*C* for the intensities of these cleavages). In addition, a rather strong cleavage can be seen in the OsO_4 profile shown in Fig. 3, at position 387 of the coding strand (red), due to the presence of a T residue immediately adjacent to the destabilizing C·C and G·G mismatches on one-half of the duplex molecules. The signal expected at position 299 was not discernible in the OsO_4 lane upon direct inspection of the fluorescence from the noncoding strand (green), which carries a mismatched T at the site corresponding to the codon 458 mutation. However, comparison with blow-up tracings of the same region of OsO_4 lanes of other individuals, as shown in Fig. 3*A Inset*, reveals that a T is indeed modified and cleaved at position 299 of the noncoding strand. This T·G mismatch, which is present in one out of four duplex molecules, is poorly reactive toward OsO_4, since the resulting peak is only slightly higher than those of matched T·A bases in the surrounding region. These are shown as five green/blue peaks in the *Inset*, which reflect the T profile of the noncoding strand from position 283 to position 316 (see, in Fig. 1*B*, the underlined T residues of the noncoding strand). The control profile (blue) shown in the *Inset*, lacking the peak at position 299, is that of an individual G·C homozygous at this polymorphic site. In fact, even interindividual variation, that is of A·T and G·C homozygotes at this polymorphic site, can be detected (data not shown). Thus, the appearance of a new T or C peak, not present in the profile of other individuals, is a sufficient diagnostic marker even if its intensity is not higher than that resulting from cleavage of the paired bases in the surrounding region. We therefore routinely superimpose and scan patient profiles in groups of four.

We then addressed the question of the thresholds at which, using this method, a mutation can be detected if present only in a fraction of the sampled cells. The patient with the cis double mutation, whose complete cleavage profile is shown in Fig. 2, displays a large number of fragments of variable intensities and thus provides a convenient way to test the limits of detection, by diluting genomic DNA of this patient with increasing amounts of control genomic DNA. Moreover, the enzymatically amplified region of the affected chromosome of this patient can be distinguished quantitatively, in the dilution series, because the T → G transversion at codon 459 destroys a recognition site for the restriction enzyme *Hgi*AI (see Fig. 1*B*). As shown in Fig. 4, genomic DNA of this patient was diluted with increasing amounts of normal DNA and enzymatically amplified. The contribution of the chromosome carrying the mutations was verified, after the first PCR amplification, by monitoring, in the dilution series, the decrease of the 588-bp fragment, which is resistant to *Hgi*AI digestion. Aliquots of each dilution series were then subjected to both chemical modifications. Upon 5-fold dilution of the DNA (i.e., one of 10 chromosomes carrying the mutations), both nucleotide mismatches shown schematically in Fig. 2 were easily detected. For sake of simplicity,

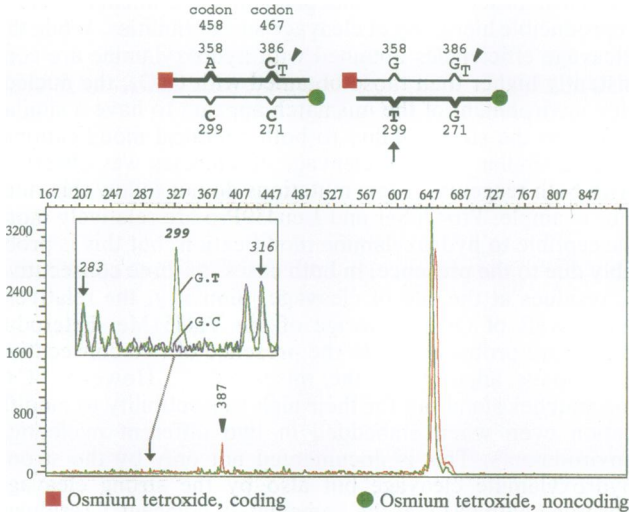

FIG. 3. Detection of a weakly reactive mispaired T residue by superimposing the cleavage profiles of different individuals. The T·G mismatch at codon 458 is due to the polymorphic G → A transition, which produces an *Hgi*AI polymorphism (see Fig. 1*B*). The second mismatch, at codon 467, is due to the presence, in this patient, of the Pro467Arg mutation (C → G). On the coding strand (red profile) adjacent to the G·G or C·C mismatches at codon 467, a T residue (arrowhead) is modified and cleaved. However, the expected cleavage at position 299 of the noncoding strand (green profile) can only be seen in the blowup of the fluorescence between positions 283 and 316 (see the underlined T residues in Fig. 1*B*). Individuals G·C homozygous (blue profile in the *Inset*) lack the fluorescence peak at position 299 but yield otherwise superimposable peaks at all paired T residues.

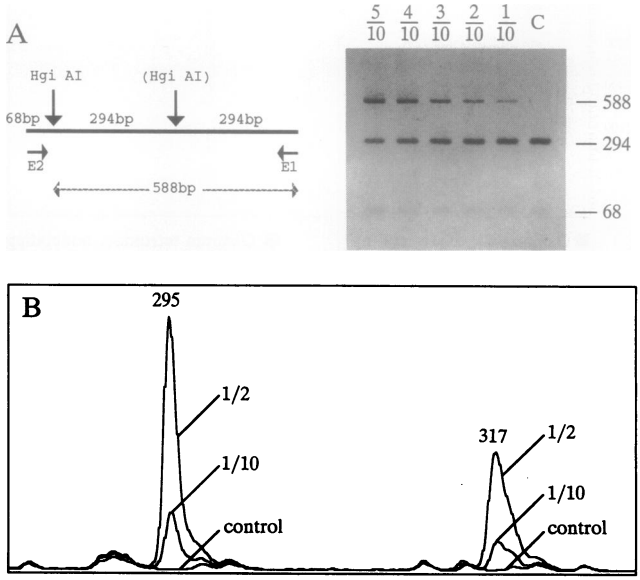

FIG. 4. Sensitivity of detection to dilution of the mutant gene. The genomic DNA of the patient with the cis double mutation, whose cleavage profile is shown in Fig. 2, was diluted with wild-type DNA. (*A*) Dilution of the mutant gene was verified after the first enzymatic amplification by monitoring the intensity of the 588-bp *Hgi*AI fragment, which is diagnostic of the mutation at codon 459 (also see Fig. 1). In the gel, lanes are designated by the dilution factor applied to the mutant gene. The control lane (C) contains wild-type DNA. (*B*) Detection of both hydroxylamine peaks at positions 295 and 317 (see the green profile in Fig. 2*A*), upon 5-fold dilution of the patient DNA (i.e., when the mutant gene is present at a 1:10 ratio).

only the hydroxylamine cleavage of the noncoding strand in the undiluted and in the 5-fold diluted DNA is shown in Fig. 4*C*. All the other cleavage products shown for this patient in Fig. 2 were, however, detected upon dilution. The hydroxylamine doublet peaks of the coding strand around position 362 (see Fig. 2*A Inset*) were barely detectable when a 1/10th dilution of the relevant chromosome was used (data not shown).

DISCUSSION

Simultaneous labeling of wild-type and mutated DNA segments with strand-specific fluorescent dyes allows efficient detection of mutations in large DNA regions. FAMA can be carried out faster than conventional CCM, with the additional benefit of the stability of the fluorescence-labeled products and the convenience of the computerized storage of cleavage profiles for subsequent comparisons. The only practical limitation, as for other PCR-based methods, is in the need to optimize the first PCR amplification step for each new DNA region. In the examples shown here, it was sufficient to optimize the choice of oligonucleotide primers and of the PCR conditions. Nested PCR has been effective for the amplification of other exons of the C1-inhibitor gene.

Simultaneous radioactive labeling of the normal and of the mutant allele has been used with the CCM method as a way to discriminate between heterozygotes and homozygotes (22), and in other studies radioactive probes were made both from normal and from patient samples, to increase the number of informative mismatches (21). Internal radioactive labeling was used in these studies, thus preventing precise localization of the mutation. A wild-type double-stranded probe, radioactively labeled at both ends, was used in other studies to reduce the number of chemical reactions (12). Our procedure differs in important ways from these and other previous approaches. First, the goal of maximizing the number of informative mismatches is achieved by labeling simultaneously the products of the wild-type and the mutant allele, but with a terminal fluorescent dye. Secondly, bichrome fluorescent PCR, in which the coding and the noncoding strands are differentially labeled, not only reduces the number of chemical reactions but also ensures the precise localization of the mutation(s). Furthermore, the observation that strand-specific background cleavage at paired positions is highly reproducible and can be used for comparisons renders detectable mismatches, which ordinarily are poorly modified and cleaved. Although FAMA is illustrated here with examples taken from a heterozygous mutation search, it can easily be adapted to detect homozygous or hemizygous mutations within large DNA fragments, by simply mixing a reference DNA with the test DNA prior to PCR amplification.

The high signal-to-noise ratio of FAMA should also open the way for its application in the detection of somatic mutations, in which the relevant chromosome is diluted within a large number of wild-type copies. The example shown in Fig. 4 indicates that cleavage signals with an average intensity are easily detected when the relevant chromosome is diluted 10-fold. By automated comparison of control profiles, we have been able to detect, at such dilutions, much weaker signals.

To further expand the scope of the method, it will be useful to optimize conditions for the resolution of DNA fragments larger than 827 bp, the upper limit tested so far, and to explore alternative cleavage methods, such as the use of mismatch repair enzymes (23), to obviate the residual hazards of toxic chemicals and the multistep timetable intrinsic to the chemical cleavage protocol.

We thank Philip Avner and Kenneth McElreavey for comments on the manuscript and Thierry Jurado for helpful discussions. This work was supported by grants from the Caisse Nationale de l'Assurance Maladie (CNAMTS), the Ministère de la Recherche et de la Technologie, the Ligue Nationale Française contre le Cancer, l'Association Française contre les Myopathies, and the Groupement de Recherches et d'Etudes sur les Génomes.

1. Grompe, M., Gibbs, R. A., Chamberlain, J. S. & Caskey, C. T. (1989) *Mol. Biol. Med.* **6**, 511–521.
2. Cotton, R. G. H. (1993) *Mutat. Res.* **285**, 125–144.
3. Smooker, P. M. & Cotton, R. G. H. (1993) *Mutat. Res.* **288**, 65–77.
4. Fischer, S. G. & Lerman, L. S. (1983) *Proc. Natl. Acad. Sci. USA* **80**, 1579–1583.
5. Sheffield, V. C., Cox, D. R., Lerman, L. S. & Myers, R. M. (1989) *Proc. Natl. Acad. Sci. USA* **86**, 232–236.
6. Costes, B., Girodon, E., Ghanem, N., Chassignol, M., Thuong, N. T., Dupret, D. & Goossens, M. (1993) *Hum. Mol. Genet.* **2**, 393–397.
7. Orita, M., Iwahana, H., Kanazawa, H., Hayashi, K. & Sekiya, T. (1989) *Proc. Natl. Acad. Sci. USA* **86**, 2766–2770.
8. Sheffield, V. C., Beck, J. S., Kwitek, A. E., Sandstrom, D. W. & Stone, E. M. (1993) *Genomics* **16**, 325–332.
9. Sarkar, G., Yoon, H.-S. & Sommer, S. S. (1991) *Nucleic Acids Res.* **20**, 871–878.
10. Cotton, R. G. H., Rodriguez, N. R. & Campbell, R. D. (1988) *Proc. Natl. Acad. Sci. USA* **85**, 4397–4401.
11. Rodriguez, N. R., Rowan, A., Smith, M. E. F., Kerr, I. B., Bodmer, W. F., Gannon, J. V. & Lane, D. P. (1990) *Proc. Natl. Acad. Sci. USA* **87**, 7555–7559.
12. Montandon, A. J., Green, P. M., Giannelli, F. & Bentley, D. R. (1989) *Nucleic Acids Res.* **17**, 3347–3358.
13. Grompe, M., Caskey, C. T. & Fenwick, R. G. (1991) *Am. J. Hum. Genet.* **48**, 212–222.
14. Anderson, M. J., Milner, C. M., Cotton, R. G. H. & Campbell, R. D. (1992) *J. Immunol.* **148**, 2795–2802.
15. Roberts, R. G., Bobrow, M. & Bentley, D. R. (1992) *Proc. Natl. Acad. Sci. USA* **89**, 2331–2335.
16. Grompe, M., Muzny, D. M. & Caskey, C. T. (1989) *Proc. Natl. Acad. Sci. USA* **86**, 5888–5892.
17. Stoppa-Lyonnet, D., Tosi, M., Laurent, J., Sobel, A., Lagrue, G. & Meo, T. (1987) *N. Engl. J. Med.* **317**, 1–6.
18. Stoppa-Lyonnet, D., Duponchel, C., Meo, T., Laurent, J., Carter, P. E., Arala-Chaves, M., Cohen, J. H. M., Dewald, G., Goetz, J., Hauptmann, G., Lagrue, G., Lesavre, P., Lopez-Trascasa, M., Misiano, G., Moraine, C., Sobel, A., Späth, P. J. & Tosi, M. (1991) *Am. J. Hum. Genet.* **49**, 1055–1062.
19. Bock, S. C., Skriver, K., Nielsen, E., Thogersen, H.-C., Wiman, B., Donaldson, V. H., Eddy, R. L., Marrinan, J., Radziejewska, E., Huber, R., Shows, T. B. & Magnusson, S. (1986) *Biochemistry* **25**, 4292–4301.
20. Carter, P., Duponchel, C., Tosi, M. & Fothergill, J. E. (1991) *Eur. J. Biochem.* **197**, 301–308.
21. Forrest, S. M., Dahl, H. H., Howells, D. W., Dianzani, I. & Cotton, R. G. H. (1991) *Am. J. Hum. Genet.* **49**, 175–183.
22. Dianzani, I., Forrest, S. M., Camaschella, C., Gottardi, E. & Cotton, R. G. H. (1991) *Am. J. Hum. Genet.* **48**, 423–424.
23. Lu, A.-L. & Hsu, I.-C. (1992) *Genomics* **14**, 249–255.